Kinetics of ^{13}CO Exchange with ^{12}CO in $[HM_3(CO)_{11}]^-$ and $[DM_3(CO)_{11}]^-$ (M = Ru, Os): Study of the Effects of Ion Pairing and Deuterium Labeling on the Exchange Process and Hydride Activation

Martin W. Payne, Daniel L. Leussing,* and Sheldon G. Shore*

Department of Chemistry, The Ohio State University, Columbus, Ohio 43210

Received July 20, 1990

Rates of exchange of ^{13}CO gas (0.1–6.0 atm) with ^{12}CO in $[HM_3(^{12}CO)_{11}]^-$ and $[DM_3(^{12}CO)_{11}]^-$ (M = Ru, Os) were determined. The appearance of ^{12}CO in the gas phase above tetrahydrofuran solutions of the cluster salts was monitored by IR spectroscopy as a function of time. Overall ^{13}CO–^{12}CO exchange occurs by two parallel pathways. A dissociative pathway, which is first order in anion and zero order in CO, dominates the exchange process. As the concentration of ^{13}CO is increased, an associative step that is first order in cluster anion and first order in CO becomes increasingly significant. Exchange reactions involving $[HRu_3(CO)_{11}]^-$ are faster than those involving $[HOs_3(CO)_{11}]^-$. With increased ion-pairing ability of the counterion of $[HRu_3(CO)_{11}]^-$, the rate of exchange increases ($PPN^+ \simeq PPh_4^+ < NEt_4^+ < K^+ < Na^+ < Li^+$), affecting, principally, the dissociative step. Similar results are observed for $[HOs_3(CO)_{11}]^-$ ($PPh_4^+ < NEt_4^+ < K^+ \simeq Na^+$). Addition of BH_3 increases the rate of exchange through the dissociative pathway. The associative pathway of exchange is related to the activation of hydride in these cluster anions when under water-gas shift reaction conditions. Examination of ^{13}CO exchange with ^{12}CO in the salts $[X][HM_3(CO)_{11}]$ ([X] = Na^+, $[PPh_4]^+$; M = Ru, Os) and $[X][DM_3(CO)_{11}]$ ([X] = Na^+, $[PPh_4]^+$; M = Ru, Os) reveals a kinetic isotope effect for the associative step, $k_2(H)/k_2(D)$ = 1.4–1.8, which can be related to the displacement by CO of the bridging to a terminal site.

I. Introduction

Under basic conditions $Ru_3(CO)_{12}$ is converted to $[HRu_3(CO)_{11}]^-$, an anion that has been studied extensively with respect to its role in homogeneously catalyzed hydroformylation[1] reactions and in particular with respect to the catalysis of the water-gas shift reaction (WGSR)[2-4] (eq 1). Earlier work[3] from this laboratory showed that

$$CO + H_2O \rightarrow CO_2 + H_2 \quad (1)$$

$[HRu_3(CO)_{11}]^-$ functions as a hydride ion donor in the presence of CO. The forward and reverse reactions of the equilibrium given in eq 2 were established.[3a,5] Consistent

$$K[HRu_3(CO)_{11}] + CO \rightleftharpoons KH + Ru_3(CO)_{12} \quad (2)$$

with this equilibrium is the formation of H_2 when CO is placed over an aqueous solution of $K[HRu_3(CO)_{11}]$. When CO is absent from the system, however, no H_2 is formed.[3b] From observations such as these and further study of the WGSR, which is catalyzed when $[HRu_3(CO)_{11}]^-$ is present in solution, a scheme was proposed[3b] that involves the interaction of CO with $[HRu_3(CO)_{11}]^-$ in an associative fashion (Scheme I). The intermediate species $[HRu_3(CO)_{12}]^-$ is believed to act as the actual hydridic species.

Scheme I

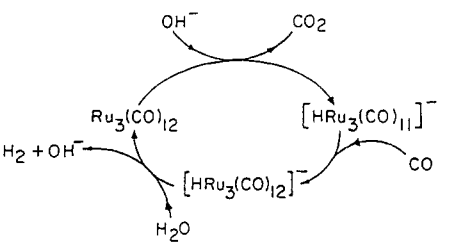

Under basic conditions[6] $Os_3(CO)_{12}$ is converted to $[HOs_3(CO)_{11}]^-$ and the system catalyzes the WGSR, but this system is less active than the corresponding ruthenium carbonylate system.[2c,7] It is likely that CO interacts with $[HOs_3(CO)_{11}]^-$ in the same fashion as it does with $[HRu_3(CO)_{11}]^-$.

The anion $[HRu_3(CO)_{11}]^-$ and $[HOs_3(CO)_{11}]^-$ have similar solid-state structures[8,9] (Figure 1) that are consistent with structures deduced from NMR spectroscopy, under limiting intramolecular slow exchange of bridging and terminal ligands.[6,10] A preliminary study[11] of ^{13}CO exchange with ^{12}CO in the clusters $[HM_3(CO)_{11}]^-$ and $[DM_3(CO)_{11}]^-$ (M = Ru, Os) in tetrahydrofuran (THF) (eq 3) indicates that ^{13}CO exchange occurs by parallel dissociative and associative exchange pathways. Although the

$$[HM_3(^{12}CO)_{11}]^- + {}^{13}CO \xrightleftharpoons{THF} [HM_3(^{12}CO)_{10}(^{13}CO)]^- + {}^{12}CO \quad (3)$$

(1) (a) Kang, H. C.; Mauldin, C. H.; Cole, T.; Slegeir, W.; Cann, K.; Pettit, R. *J. Am. Chem. Soc.* **1977**, *99*, 8323. (b) Laine, R. M. *J. Am. Chem. Soc.* **1978**, *100*, 6451. (c) Suss-Fink, G. *J. Organomet. Chem.* **1980**, *193*, C20. (d) Suss-Fink, G.; Reiner, J. *J. Mol. Catal.* **1982**, *16*, 231. (e) Suss-Fink, G.; Herrmann, G. *J. Chem. Soc., Chem. Commun.* **1985**, 735.

(2) (a) Ford, P. C.; Rinker, R. G.; Ungermann, C.; Laine, R. M.; Landis, V.; Moya, S. A. *J. Am. Chem. Soc.* **1978**, *100*, 4595. (b) Ungermann, C.; Landis, V.; Moya, S. A.; Cohen, H.; Walker, H.; Pearson, R. G.; Rinker, R. G.; Ford, P. C. *J. Am. Chem. Soc.* **1979**, *101*, 5922. (c) Ford, P. C.; Ungermann, C.; Landis, V.; Moya, S. A.; Rinker, R. G.; Laine, R. M. *Adv. Chem. Ser.* **1979**, *No. 173*, 81. (d) Ford, P. C. *Acc. Chem. Res.* **1981**, *14*, 31.

(3) (a) Bricker, J. C.; Nagel, C. C.; Shore, S. G. *J. Am. Chem. Soc.* **1982**, *104*, 1444. (b) Bricker, J. C.; Nagel, C. C.; Bhattacharyya, A. A.; Shore, S. G. *J. Am. Chem. Soc.* **1985**, *107*, 377.

(4) Dombek, B. D. *J. Am. Chem. Soc.* **1981**, *103*, 6508.

(5) Bricker, J. B.; Payne, M. W.; Shore, S. G. *Organometallics* **1987**, *6*, 2545.

(6) Eady, C. R.; Johnson, B. F. G.; Lewis, J.; Maletesta, M. C. *J. Chem. Soc., Dalton Trans.* **1978**, 1358.

(7) Pettit, R.; Cann, K.; Cole, T.; Mauldin, C. H.; Slegeir, W. *Adv. Chem. Ser.* **1979**, *No. 173*, 121.

(8) Johnson, B. F. G.; Lewis, J.; Raithby, P. R.; Suss, G. *J. Chem. Soc., Dalton Trans.* **1979**, 1356.

(9) Siriwardane, U. Ph.D. Dissertation, The Ohio State University, Columbus, OH, 1985.

(10) Bhattacharyya, A. A.; Nagel, C. C.; Shore, S. G. *Organometallics* **1983**, *2*, 1187.

(11) Payne, M. W.; Leussing, D. L.; Shore, S. G. *J. Am. Chem. Soc.* **1987**, *109*, 617.

0276-7333/91/2310-0574$02.50/0

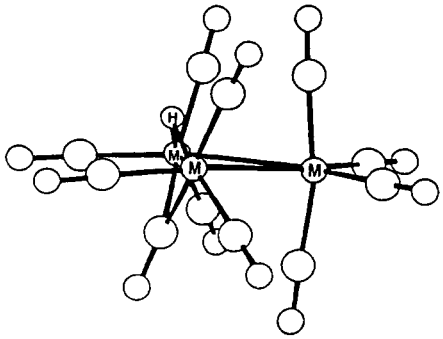

Figure 1. Structure of $[HM_3(CO)_{11}]^-$ (M = Ru,[6] Os[7]).

dissociative step dominates the overall exchange process, the associative pathway is the one that is directly related to the catalysis of the WGSR of these clusters.

To study the effects of ion pairing and to obtain additional details on the effect of deuterium labeling, we have studied further the exchange of ^{13}CO with ^{12}CO in these trinuclear cluster anions in THF (eq 3). Reported here are details of our earlier work on ^{12}CO–^{13}CO as well as more recent results. This work represents the first detailed kinetic investigation of ^{13}CO–^{12}CO exchange involving a metal cluster anion. It is also one of the very few[12] detailed kinetic studies of ligand exchange or substitution with any metal cluster anion.

II. Experimental Section

A. Solvents and Starting Materials. Carbon monoxide, 99% ^{13}C enriched (Isotec, Inc.), was used as received. THF, Et_2O, and glyme were distilled from and stored over sodium–benzophenone ketyl. Hexane and pentane were stirred over concentrated H_2SO_4 for 2 days and distilled from CaH_2 into a storage bulb equipped with a Kontes Teflon stopcock. CH_2Cl_2 and CH_3CN were distilled from CaH_2 into a storage bulb equipped with a Kontes Teflon stopcock. Deionized doubly distilled H_2O was used after through degassing by three freeze–pump–thaw cycles on the vacuum line. $Os_3(CO)_{12}$ (Strem Chemical Co.) was used as received. $Ru_3(CO)_{12}$ was prepared from $RuCl_3$ (Aldrich Chemical Co.) and CO (Matheson) by use of a previously reported procedure.[13] B_2H_6 was prepared and purified according to a standard method.[14] It was stored in a Pyrex tube with a glass high-vacuum stopcock at −196 °C.

The salts $Li[HRu_3(CO)_{11}]$,[15] $Na[HRu_3(CO)_{11}]$,[8] $K[HRu_3(CO)_{11}]$[3b] $K[DRu_3(CO)_{11}]$,[3b] $Na[DRu_3(CO)_{11}]$, $[Et_4N][HRu_3(CO)_{11}]$,[8] $[PPN][HRu_3(CO)_{11}]$,[8,16] and $[PPh_4][HRu_3(CO)_{11}]$[17] were prepared according to recipies in the literature. $[PPh_4][DRu_3(CO)_{11}]$ was prepared from the metathesis reaction of $Na[DRu_3(CO)_{11}]$ with $[PPh_4]Br$ in a THF–CH_2Cl_2 (1:1) solvent mixture. The salts $[PPh_4][HOs_3(CO)_{11}]$, $[NEt_4][HOs_3(CO)_{11}]$, $Na[HOs_3(CO)_{11}]$, $K[HOs_3(CO)_{11}]$, and their deuterated counterparts were prepared by procedures very similar to those employed in the preparations of the $[HRu_3(CO)_{11}]^-$ analogues.

B. Apparatus. A Pyrex glass high-vacuum system similar to that described by Shriver and Drezdzon[18] was used for the quantitative manipulation of volatile and air-sensitive compounds. Manipulations of nonvolatile air-sensitive compounds were carried out in a controlled-atmosphere glovebox.

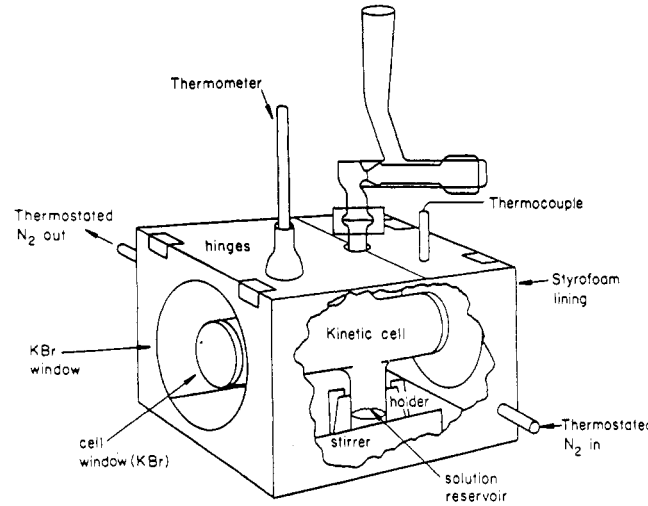

Figure 2. IR cell and thermostated container.

Figure 2 depicts the IR cell used for rate measurements in a thermostated box, which was placed in the sample compartment of the IR spectrometer. This cell is constructed from Pyrex glass with a path length of 12 cm, and 30 mm o.d. KBr windows, 32 × 3 mm, are employed. The solution reservoir of the cell is 30 mm in diameter and 40 mm in length. A Teflon-coated stirbar resides in this reservoir. A 9-mm Fischer-Porter Solv-Seal joint, for addition of reactants, is attached to the cell directly above the solution reservoir. It is sealed by a vacuum adapter equipped with a Kontes Teflon 4-mm stopcock. The volume of the cell, 96.5 mL, was calculated from pressure and temperature measurements of known amounts of CO_2 in the cell. After each kinetic run the cell was disassembled, cleaned, and reassembled. The thermostated box is surrounded on all sides (except the bottom) by a $^1/_2$-in. layer of insulating Styrofoam. An air-driven magnetic stirrer for stirring reaction solutions is in the bottom of the box, and the air flow rate is monitored by a Kontes Flow-Watchman flow meter. An optimum range of stirring rates that give reproducible kinetic data was determined and monitored by means of the flow meter. Each end of the box has a 2-in. circular hole, which is sealed with a 49 × 6 mm polished KBr window glued in place. The box is maintained at a constant desired temperature by a stream of nitrogen gas, which passes through a heated or cooled coil of copper tubing and then passes through the box. The coil is heated by insulated nichrome wire connected to a variable-voltage transformer. For box temperature lower than room temperature the coil is cooled by immersing it in ice water. The thermostated gas is transmitted to the box by means of insulated vacuum tubing, and the temperature of the box is continuously monitored by a thermocouple probe connected to a recording potentiometer.

The ^{13}CO delivery system to the IR cell contains a mercury in-glass manometer with a range of 2900 Torr, a 100-psi Bourdon pressure gauge, and a source of ^{13}CO. For pressures above 2700 Torr the pressure gauge is employed for pressure measurements of ^{13}CO.

C. Solubility Determination of CO. The solubility of CO in THF was determined with use of a variation of the apparatus and methods of Rivas and Prausnitz.[19] A full description of the apparatus and the calculation of the solubility values are given elsewhere.[20] The amount of CO dissolved in a known amount of THF was determined at 25 and 30 °C in the pressure range 0.1–2.0 atom. Plots of the total CO pressure vs molarity of CO in THF proved to be linear at both 25 and 30 °C. Values of CO solubility are given in moles per liter per atmosphere and are 0.0109 ± 0.0003 mol/(L atm) at 25 °C and 0.0117 ● 0.0003 mol/(L atm) at 30 °C. These units have been suggested to be the most

(12) (a) Anstock, M.; Taube, D.; Gross, D. C.; Ford, P. C. *J. Am. Chem. Soc.* **1984**, *106*, 3696. (b) Taube, D. J.; Ford, P. C. *Organometallics* **1986**, *5*, 99. (c) Taube, D. J.; Rokicki, A.; Anstock, A.; Ford, P. C. *Inorg. Chem.* **1987**, *26*, 526.

(13) Eady, C. R.; Jackson, P. F.; Johnson, B. F. G.; Lewis, J.; Malatesta, M. C.; McPartlin, M.; Nelson, W. J. H. *J. Chem. Soc., Dalton Trans.* **1980**, 383.

(14) Toft, M. A.; Leach, J. B.; Himpsl, F. L.; Shore, S. G. *Inorg. Chem.* **1982**, *21*, 1952.

(15) Schick, K. P.; Jones, N. L.; Sekula, P.; Boag, N. M.; Labinger, J. A.; Kaesz, H. D. *Inorg. Chem.* **1984**, *23*, 2204.

(16) Lavigne, G.; Lugan, N.; Bonnet, J. J. *Inorg. Chem.* **1987**, *26*, 2345.

(17) Sakakura, T.; Kobayashi, T.; Tanaka, M. *C1 Mol. Chem.* **1985**, *1*, 219.

(18) Shriver, D. F.; Drezdzon, M. A. *The Manipulation of Air Sensitive Compounds*, 2nd ed.; Wiley: New York, 1986.

(19) Rivas, O. R.; Prausnitz, J. M. *Ind. Eng. Chem. Fundam.* **1979**, *18*, 289.

(20) Payne, M. W. Ph.D. Dissertation, The Ohio State University, Columbus, OH, 1987.

convenient for kinetic studies.[12] Our experimental values are consistent with estimates of the solubility calculated by Ford.[12b] It is worth noting that the solubility of CO in THF seems to increase with an increase in temperature. In a similar study by Calderazzo and Cotton[21] an increase in CO solubility in ethers was detected. For the analysis of kinetic data, all values for CO solubility in THF at temperatures other than 25 and 30 °C were determined by a least-squares plot of solubility vs temperature.

D. Determination of Reaction Rate. Generally between 0.01 and 0.04 mmol (9–20 mg) of a $[HM_3(CO)_{11}]^-$ salt (M = Ru, Os) was used for a rate study. Rates were observed in the range 20–35 °C and 0.1–6.0 atm of ^{13}CO.

In the drybox the metal carbonyl anion was weighed out on an analytical balance. A funnel was placed in the top junction of the gas IR cell, and the compound was washed by THF to the bottom reservoir of the cell. The top of the gas IR cell was fitted with a vacuum adapter, and the THF was pumped away under vacuum, leaving behind the solid cluster salt in the bottom of the reservoir of the cell. By the use of a −78 °C slush bath, THF was condensed into the calibrated reservoir to a mark denoting 9.00 mL of solution. The cell was warmed to room temperature and placed in the thermostated box in the FTIR spectrometer sample compartment. Then the box was sealed at the top and thermostated N_2 was passed through the box until the desired temperature in the box was reached and maintained. The stirring motor was then started, and the ^{13}CO gas delivery system was attached and wired to the top of the gas IR cell. At this time a background IR spectrum was obtained. The ^{13}CO delivery system up to the IR cell stopcock was evacuated. The stopcock to the vacuum pump was closed, and the stopcock to the cell was opened. The vapor pressure of the THF was measured on the manometer before ^{13}CO delivery and was subtracted from the total pressure after ^{13}CO was added. A measured amount of ^{13}CO gas (in Torr) was added, and the data acquisition program of the FTIR spectrometer was activated. Four sample scans, over a period of 3 s, were taken at each sampling interval, which was computer-controlled. Sampling intervals were 20 s apart for the first 5 min, 30 s apart for the next 5 min, 1 min apart for the next 10 min, and 5 min apart thereafter. During the collection of rate data, the temperature was continuously monitored on a chart recorder. If there was a change in temperature greater than ±0.1 °C, the experiment was abandoned. When BH_3 was measured volumetrically and condensed into the IR cell, the reservoir of the cell was cooled to −196 °C.

E. Data Reduction. Once a set of rate data was collected, it was processed with use of the background recorded at the beginning of the experiment. A plot of absorbance vs time conformed to an exponential decay, as is typical for exchange reactions of this type. The absorbance vs time data for the absorbance of ^{12}CO at 2171 cm^{-1} was then entered into a standard nonlinear curve-fitting program, MINUIT.[22] From this program, the value for the observed rate constant k_{obs} was determined: $A_t = A + A_i e^{-k_{obs}t}$, where A_t and A_i are the absorbances at time t and infinite time; A_i is the magnitude of the absorbance change from $t = 0$ to $t = \infty$.

The rate constants for exchange were obtained from k_{obs} with use of the McKay equation[23] for isotopic ligand exchange. A statistical correction was used in calculations of rates since intermolecular CO exchange is slower than intramolecular scrambling of the 11 CO's in the clusters in the temperature range that rate data were collected.[55] From the rate data and the calculated concentrations of CO and cluster, the order of the reaction and the rate constants were determined with use of standard treatments of rate data. Activation parameters, $\Delta H^\ddagger$ and $\Delta S^\ddagger$, were determined by use of Arrhenius plots of the natural logarithm of the rate constant vs $1/T$ (K).

F. Reactions of $K[HRu_3(CO)_{11}]$ and $K[DRu_3(CO)_{11}]$ with CO in H_2O. The reaction of $K[HRu_3(CO)_{11}]$ with CO and H_2O was performed in a manner similar to the method of Bricker et al.[3b] The reaction temperature was maintained at 55 °C for 5 h, after which the reaction solution was frozen at −78 °C and the gas above the solution was measured with the aid of a Toepler pump. The gas above the solution was analyzed and found to contain 70.1% of 1 molar equiv of H_2 gas per initial mole of $[HRu_3(CO)_{11}]^-$. The reaction of $K[DRu_3(CO)_{11}]$ with CO and H_2O was performed under identical conditions, and 76.8% of 1 molar equiv of HD per initial mole of $[DRu_3(CO)_{11}]^-$ was found above the solution after 40.5 h at 55 °C.

(21) Calderazzo, F.; Cotton, F. A. *Inorg. Chem.* **1962**, *1*, 30.
(22) James, F.; Roos, M. *Comput. Phys. Commun.* **1974**, *10*, 343.
(23) McKay, H. A. C. *J. Am. Chem. Soc.* **1943**, *65*, 702.

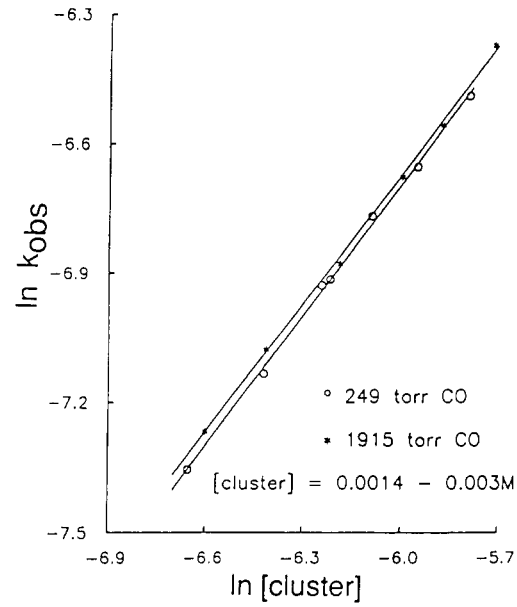

Figure 3. Plot of ln k_{obs} vs ln $[Na[HRu_3(CO)_{11}]]$ at two different pressures of ^{13}CO.

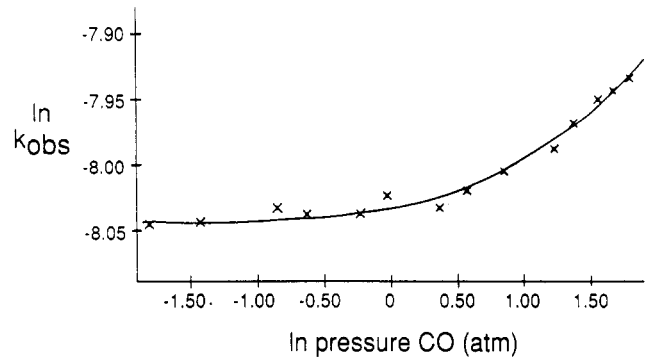

Figure 4. Plot of ln k_{obs} vs ln (CO pressure) for $[PPh_4][HRu_3(CO)_{11}]$ in THF.

III. Results and Discussion

A. Rate Law. Exchange reactions between ^{13}CO gas and ^{12}CO in salts of $[HM_3(CO)_{11}]^-$ and $[DM_3(CO)_{11}]^-$ (M = Ru, Os) in THF solutions were studied with IR spectroscopy. The rate of ^{12}CO enrichment of the gas phase above the reaction solution was followed as a function of time.

The rate of exchange is first order with respect to cluster concentration for all of the above systems. Plots of ln k_{obs} vs ln [cluster] at two different constant pressures of ^{13}CO have slopes of 1.00 ± 0.02. A typical plot is shown in Figure 3.

The first-order dependence on cluster concentration is independent of the cation used. The rate is a function of which cation and cluster anion pair is employed. Plots of ln k_{obs} vs ln pressure (Torr) of ^{13}CO at constant cluster concentrations, for all of the above systems, show that at ^{13}CO pressures less than 1 atm, the rate of exchange is almost independent of ^{13}CO pressure. As the pressure of ^{13}CO and therefore its concentration in solution increases, the slope increases markedly. A typical plot is shown in Figure 4.

Table I. Rate Constants k_1 (s^{-1}) and k_2 (s^{-1} M^{-1}) at 25 °C in THF

	$[HRu_3(CO)_{11}]^-$		$[DRu_3(CO)_{11}]^-$			
cation	k_1	k_2	k_1	k_2	$k_1(H)/k_1(D)$	$k_2(H)/k_2(D)$
$[PPN]^+$	0.24 (1)	0.55 (3)				
$[PPh_4]^+$	0.253 (4)	0.540 (6)	0.247 (5)	0.387 (10)	1.02 (4)	1.40 (1)
$[NEt_4]^+$	0.36 (1)	0.51 (4)				
K^+	0.55 (2)	0.47 (3)				
Na^+	0.62 (2)	0.43 (4)	0.52 (5)	0.26 (2)	1.2 (2)	1.7 (4)
Li^+	0.83 (1)	0.41 (4)				
	$[HOs_2(CO)_{11}]^-$		$[DOs_3(CO)_{11}]^-$			
cation	k_1	k_2	k_1	k_2	$k_1(H)/k_1(D)$	$k_2(H)/k_2(D)$
$[PPh_4]^+$	0.0212 (10)	0.043 (9)	0.0211 (15)	0.029 (7)	1.00 (12)	1.5 (5)
$[NEt_4]^+$	0.0430 (51)	0.033 (8)				
K^+	0.098 (7)	0.020 (5)				
Na^+	0.098 (4)	0.022 (5)	0.095 (6)	0.012 (4)	1.0 (1)	1.8 (1.3)

Table II. Activation Parameters ΔH^* (kcal/mol) and ΔS^* (cal/(mol K))

salt	ΔH_1^*	ΔH_2^*	ΔS_1^*	ΔS_2^*
$[PPh_4][HRu_2(CO)_{11}]$	19.8 (6)	14.1 (5)	5.31 (1.54)	-8.00 (1.73)
$Na[HRu_3(CO)_{11}]$	18 (1)	15 (1)	2.5 (1.7)	-10 (2)
$[PPh_4][HOs_3(CO)_{11}]$	23.9 (7)	20 (3)	13.9 (2.3)	-10 (3)
$Na[HOs_3(CO)_{11}]$	22.2 (6)	20 (4)	11.3 (1.6)	-10 (4)

An overall rate expression for the forward exchange reaction is given by eq 4, where the brackets denote con-

$$\text{rate} = k_1[\text{cluster}] + k_2[\text{cluster}][\text{CO}] \quad (4)$$

centration in moles per liter. Plots of rate/[cluster] vs [CO] are linear (Figure 5), which is in accord with this expression. Rate constants are given in Table I. Enthalpies and entropies of activation are given in Table II.

$[HRu_3(CO)_{11}]^-$ exchanges carbon monoxide about 1 order of magnitude more rapidly than $[HOs_3(CO)_{11}]^-$ under equvalent conditions. Because of the low solubility of CO in THF (about 0.01 mol/(L atm)) the first-order-term, dissociative pathway (eqs 5 and 6) dominates the overall

$$[HM_3(^{12}CO)_{11}]^- \underset{k_{-1}}{\overset{k_1}{\rightleftharpoons}} [HM_3(^{12}CO)_{10}]^- + {}^{12}CO \quad (5)$$

$$[HM_3(^{12}CO)_{10}]^- + {}^{13}CO \underset{k'_1}{\overset{k'_{-1}}{\rightleftharpoons}} [HM_3(^{12}CO)_{10}(^{13}CO)]^- \quad (6)$$

$$[HM_3(^{12}CO)_{11}]^- + {}^{13}CO \underset{k_{-2}}{\overset{k_2}{\rightleftharpoons}} [HM_3(^{13}CO)(^{12}CO)_{11}]^- \quad (7)$$

$$[HM_3(^{13}CO)(^{12}CO)_{11}]^- \underset{k'_2}{\overset{k'_{-2}}{\rightleftharpoons}} [HM_3(^{13}CO)(^{12}CO)_{10}]^- + {}^{12}CO \quad (8)$$

M = Ru, Os

exchange process, while the second-order-term, associative pathway (eqs 7 and 8) becomes significant only at high pressures. The positive values of ΔS_1^* and the negative values of ΔS_2^* are consistent with dissociative and associative processes, respectively. The presence of a dissociative pathway is consistent with a proposal of Darensbourg.[24]

Ford and co-workers[12b] observed a dissociative pathway for the forward reaction in the PPh_3–CO exchange reaction shown in eq 9. They also showed[12b,25] that intimate solvent

$$[PPN][HRu_3(CO)_{11}] + PPh_3 \underset{}{\overset{k_1}{\rightleftharpoons}} [PPN][HRu_3(CO)_{10}(PPh_3)] + CO \quad (9)$$

(THF) interaction with the intermediate complex is not

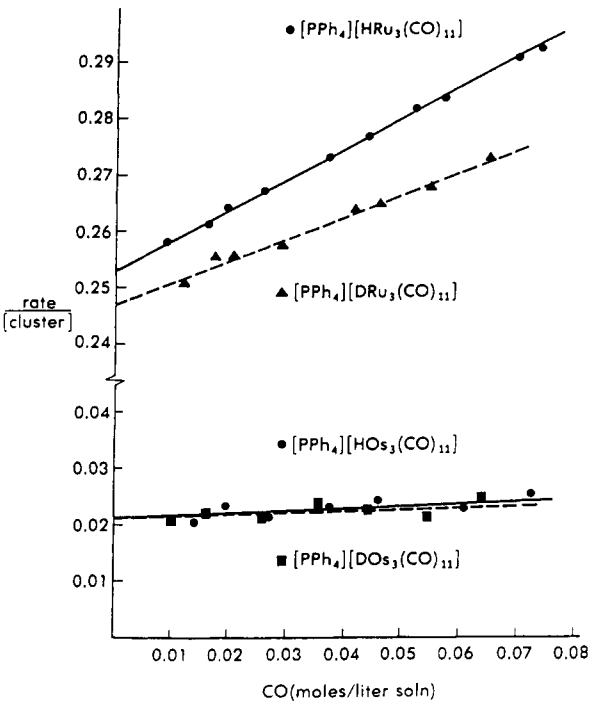

Figure 5. Plot of rate/[cluster] vs [CO] in THF.

likely and that the activation volume, ΔV^*, supports a purely dissociative step: ΔV^* is essentially equal to the molar volume of liquid CO. Consistent with Ford's and our rate evidence for a dissociative step, we find that CO is removed when $[HRu_3(CO)_{11}]^-$ is continuously pumped on for an extended period of time, leaving behind as the initial product the proposed[20] species "$[HRu_3(CO)_{10}]^-$", which slowly disproportionates into $[H_3Ru_4(CO)_{12}]^-$, $[H_2Ru_4(CO)_{12}]^{2-}$, and $[Ru_6(CO)_{18}]^{2-}$. Addition of CO to "$[HRu_3(CO)_{10}]^-$" results in the regeneration of $[HRu_3(CO)_{11}]^-$. We have recently demonstrated that $H_2Ru_6(CO)_{18}$ loses CO to form $H_2Ru_6(CO)_{17}$.[54]

Rate constants k_1 for the dissociative step involving $[HRu_3(CO)_{11}]^-$ salts are larger than values for $[HOs_3(CO)_{11}]^-$ salts with corresponding counterions, consistent with the fact that ruthenium–carbon bonds are weaker than osmium–carbon bonds.[26] Accordingly, values of ΔH_1^* are larger for the osmium cluster than for the ruthenium cluster. Equivalent observations have been made in studies of the displacement of CO from $M_3(CO)_{12}$ (M = Fe, Ru, Os) by phosphines.[27,28]

(24) Darensbourg, D. J.; Pala, M.; Waller, J. *Organometallics* **1983**, *2*, 1285.
(25) Taube, D. J.; Van Eldik, R.; Ford, P. C. *Organometallics* **1987**, *6*, 125.
(26) Housecroft, C. E.; O'Neill, M. E.; Wade, K.; Smith, B. C. *J. Organomet. Chem.* **1981**, *213*, 35.
(27) Brodie, N.; Poe, A.; Sekhar, V. *J. Chem. Soc., Chem. Commun.* **1985**, 1090.

Table III. Effect of BH_3 on Rate Constants k_1 (s^{-1}) and k_2 (s^{-1} M^{-1}) of $[HRu_3(CO)_{11}]^-$ Salts in THF at 25 °C

cation	k_1	$k_1(BH_3)$	$k_1(BH_3)/k_1$	k_2	$k_2(BH_3)$	$k_2(BH_3)/k_2$
$[PPh_4]^+$	0.253 (4)	1.1 (1)	4.3	0.540 (6)	0.55 (3)	1.0 (1)
K^+	0.55 (2)	1.2 (1)	2.2	0.47 (3)	0.52 (6)	1.1 (2)
Na^+	0.62 (2)	1.0 (1)	1.6	0.43 (4)	0.44 (5)	1.0 (3)

Rate constants k_2 for the associative step are 1 order of magnitude greater for salts of the ruthenium cluster anion than the corresponding salts of the osmium cluster anion. Ligand-exchange reactions with $M_3(CO)_{12}$ (M = Ru, Os)[27] show a similar trend in the k_2 rate constants. Activation parameters for the ^{13}CO-^{12}CO exchange reported here are within the range of observed values for associative ligand exchange involving metal clusters[27-32] and also mononuclear metal complexes.[33]

Parallel dissociative and associative pathways are common in ligand-exchange reactions for a number of different types of metal clusters.[27-29] The relative importance of the individual exchange pathway is a function of the system studied. While qualitative data are available on ligand substitution reactions involving metal cluster anions,[11,12,25,34-37] there have been only three studies,[11,12,25] including the preliminary results of the present one, in which the kinetics of ligand exchange of a cluster anion have been examined in any detail. That the present study shows both associative and dissociative pathways for ^{13}CO–^{12}CO exchange, as distinguished from Ford's demonstration of only dissociative PPh_3–CO exchange for $[HRu_3(CO)_{11}]^-$, is possibly related to the relative steric requirements of the ligands.

B. Effects of Ion Pairing. Certain salts of $[HRu_3(CO)_{11}]^-$ exhibit ion pairing in several solvents.[15,17] In THF a solvent-separated ion pair and a contact ion pair are found to exist between the solvated cation and the oxygen of the bridging carbonyl in the anion. Bridging carbonyl stretching frequencies[15,17] have been related to the types of ion pairing present in solution. We find ion-pairing behavior for the salts of $[HOs_3(CO)_{11}]^-$ in THF (Figure 6) to be similar to that of $[HRu_3(CO)_{11}]^-$ salts. With the $[PPh_4]^+$ cation only one bridging carbonyl band is present in the IR spectrum. This band represents the solvent-separated ion pair. Cations that tend to form intimate ion pairs, as well as contact ion pairs, produce a second-band at lower frequency in the IR spectrum.

Kinetic measurements on salts of $[HRu_3(CO)_{11}]^-$ and $[HOs_3(CO)_{11}]^-$ show that the rates of carbon monoxide exchange are affected by ion pairing (Table I). Activation parameters for the exchange of ^{13}CO with $Na[HM_3(^{12}CO)_{11}]$ and $[PPh_4][HM_3(CO)_{11}]$ (M = Ru, Os) were determined (Table II).

The principal effect of ion pairing is on the dissociative exchange pathway. The dissociative rate constant, k_1, increases with the strength of ion pairing ($[PPN]^+ \simeq [PPh_4]^+ < [NEt_4]^+ < K^+ < Na^+ < Li^+$) for $[HRu_3(CO)_{11}]^-$. Although not studied in as much detail, results appear to be similar for the salts of $[HOs_3(CO)_{11}]^-$ (Table I). Dissociative ligand exchange involving ion-paired mononuclear carbonylates show similar trends and relative differences in rate constants.[38-42]

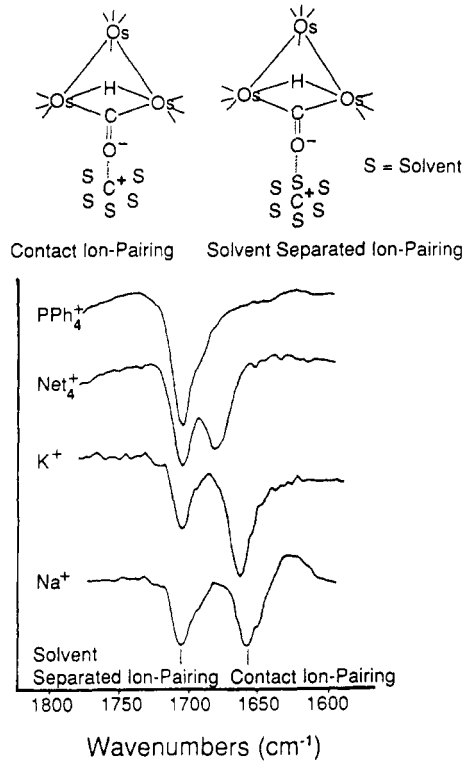

Figure 6. IR spectra of the bridging carbonyl region of $[HOs_3(CO)_{11}]^-$ in THF at 25 °C as salts of $[PPh_4]^+$ (1705 cm^{-1}), $[NEt_4]^+$ (1705, 1682 cm^{-1}), K^+ (1704, 1659 cm^{-1}), and Na^+ (1702, 1658 cm^{-1}).

The effect of ion pairing is enhanced when the leaving ligand is trans to the ion-paired carbonyl.[42] In the structures of $[HM_3(CO)_{11}]^-$ (M = Ru, Os) the two equivalent metal centers are pseudooctahedral (Figure 1). Ford's observations on phosphine substitution[12b,25] suggest that in the present case the two carbonyls trans to the bridging CO are most likely to be affected by ion pairing of the bridging carbonyl. Owing to a decrease in π back-bonding, loss of CO from $[HRu_3(CO)_{11}]^-$ will cause the electron density on the cluster to increase, resulting in a stronger product ion pair. This product stabilization will be manifested by a lowering of the barrier to reaction.[43]

The effect of a Lewis acid on the dissociative exchange pathway was examined by the introduction of BH_3 to the reaction solution. It was anticipated that BH_3 would coordinate to the bridging carbonyl oxygen[44] and affect the

(28) Shojaie, A.; Atwood, J. D. *Organometallics* **1985**, *4*, 187.
(29) Poe, A.; Twigg, M. V. *J. Chem. Soc., Dalton Trans.* **1974**, 1860.
(30) Bor, G.; Dietler, U. K.; Pino, P.; Poe, A. *J. Organomet. Chem.* **1978**, *154*, 301.
(31) Malik, S. K.; Poe, A. *Inorg. Chem.* **1979**, *18*, 1241.
(32) Poe, A.; Twigg, M. V. *Inorg. Chem.* **1974**, *13*, 2982.
(33) Howell, J. A. S.; Burkinshaw, P. M. *Chem. Rev.* **1983**, *83*, 557.
(34) Jungbluth, H.; Suss-Fink, G.; Pellinghelli, M. A.; Tiripicchio, A. *Organometallics* **1989**, *8*, 925.
(35) Malatesta, L.; Caglio, G. *J. Chem. Soc., Chem. Commun.* **1967**, 420.
(36) Chini, P.; Cavalieri, A.; Martinengo, S. *Coord. Chem. Rev.* **1972**, *8*, 3.
(37) Cooke, C. G.; Mays, M. J. *J. Organomet. Chem.* **1974**, *74*, 449.
(38) Darensbourg, M. Y.; Jimenez, P.; Sackett, J. R.; Hanckel, J. M.; Kump, R. L. *J. Am. Chem. Soc.* **1982**, *104*, 1521.
(39) Collman, J. P.; Cawse, J. N.; Brauman, J. I. *J. Am. Chem. Soc.* **1972**, *94*, 5905.
(40) Darensbourg, M. Y.; Burns, D. *Inorg. Chem.* **1974**, *13*, 2970.
(41) Darensbourg, M. Y.; Darensbourg, D. J.; Barros, H. L. C. *Inorg. Chem.* **1978**, *17*, 297.
(42) Darensbourg, M. Y.; Hanckel, J. M. *Organometallics* **1982**, *1*, 82.
(43) (a) Marcus, R. A. *J. Phys. Chem.* **1966**, *72*, 891. (b) Marcus, R. A. *J. Am. Chem. Soc.* **1969**, *91*, 7224.
(44) Reduction of $[HRu_3(CO)_{11}]^-$ by an equivalent amount of BH_3 in THF under similar conditions is very slow compared to the reaction time for a typical exchange measurement.

rate in the same manner that contact ion pairing does. One equivalent of BH_3, in the form of B_2H_6,[45] was added to the THF solutions of the Na^+, K^+, and $[PPh_4]^+$ salts of $[HRu_3(CO)_{11}]^-$, and the rate of reaction was monitored as before. The dissociative rate constants, k_1, in the presence and absence of BH_3 are given in Table III.

These results show that the dissociative rate constant, k_1, is essentially independent of the cation for all of the BH_3-assisted exchange reactions studied, but for a specific cation, k_1 is 1.6–4.3 times larger than that for the non-BH_3-assisted exchange reaction. The effect of BH_3 on the k_1 rate constant is greatest for the $[PPh_4]^+$ salt, the salt that consists of essentially solvent-separated ion pairs in solution. With the increasing ability of the cation to form contact ion pairs with the cluster anion, the effect of BH_3 on increasing the dissociative exchange rate is diminished, probably because of the increasing competition with the cation for coordination with the bridging carbonyl oxygen atom.

The effect of ion pairing on the k_2 rate constants appears to be slight and opposite to the effect on k_1 (Table I). Within experimental error, for a given salt of $[HRu_3(CO)_{11}]^-$, addition of BH_3 has no effect on the associative rate constant k_2 (Table III).

C. Catalysis of the Water-Gas Shift Reaction. In the reaction of $[HRu_3(CO)_{11}]^-$ with CO and H_2O in the water-gas shift reaction, the steps given in eqs 10 and 11

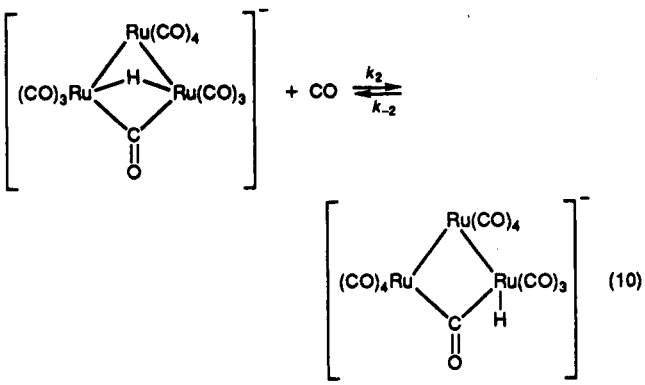

(10)

$$[HRu_3(CO)_{12}]^- + H_2O \xrightarrow{k_3} Ru_3(CO)_{12} + H_2 + [OH]^- \quad (11)$$

have been proposed.[3f,g] The catalytic cycle (Scheme I) is completed by reaction of $Ru_3(CO)_{12}$ with $[OH]^-$ to regenerate $[HRu_3(CO)_{11}]^-$.

Evidence in support of the proposed associative step of the WGSR (eq 10) is given by the associative step observed in the present study (eq 7) and the inhibiting effect of deuterium labeling on this step (Table I). The poorer ability of $[HOs_3(CO)_{11}]^-$ to participate in an associative CO-exchange pathway accounts at least in part, for its activity being lower than that of $[HRu_3(CO)_{11}]^-$ in the catalysis of the WGSR. The larger size of Os and its greater metal–carbon bond strength are expected to favor an associative path for Os relative to Ru. However, if the associative path also involves a shift of bridging H to form an Os–H two-center bond, then an Os–H–Os bridge bond stronger than an Ru–H–Ru bond would account for the step for $[HOs_3(CO)_{11}]^-$ being slower than the step for $[HRu_3(CO)_{11}]^-$.

As indicated in eq 10, the addition of CO to the trinuclear anion is believed to induce opening of the hydrogen bridge bond to form a terminal hydride that functions as H^- in the presence of a protonic source.[3] Displacement of a bridging ligand to a terminal position on an Os atom upon addition of CO to $H_2Os_3(CO)_{10}$ has been observed.[46] In the systems studied here, subsequent motion of the hydrogen to form a metal formyl might also occur. Although the transient complex $[Ru_3(CO)_{11}(CHO)]^-$ has been observed,[47] it decomposes above −50 °C. Such a formyl would be hydridic[48] and would also be expected to generate H_2 in the presence of a proton source. In this study the metal–hydride and metal–formyl pathways are kinetically indistinguishable.

The dominant effect[49] of a deuterium label (Table I, Figure 5) is to decrease, significantly, k_2. Ratios of $k_2(H)/k_2(D)$, 1.4–1.8, are consistent with our suggestion[3] that in the associative step CO addition is accompanied by movement of the bridging hydrogen atom to a terminal position. These values are in accord with k_H/k_D ratios determined for processes involving the movement of a bridge hydrogen to a terminal position in similar types of clusters.[50]

The overall reaction for the WGSR is expressed by eq 12. Since $[HRu_3(CO)_{12}]^-$ is a reactive intermediate that

$$[HRu_3(CO)_{11}]^- + H_2O + CO \xrightarrow{k_4} Ru_3(CO)_{12} + H_2 + [OH]^- \quad (12)$$

does not reach detectable concentrations during the course of the reaction, the steady-state approximation[51] can be evoked and from eqs 10–12 the rate constant k_4 can be given as eq 13. The value of k_4 is estimated to be about

$$k_4 = \frac{k_3 k_2}{k_{-2} + k_3} \quad (13)$$

1×10^{-3} M^{-1} s^{-1} for the liberation of H_2 (eq 12) from an aqueous solution 0.001 M in $K[HRu_3(CO)_{11}]$ at 25 °C under 1 atm of CO, on the basis of earlier reported data,[3b] and [CO] set equal to its solubility in H_2O.[52] The low value of k_4 compared to that of k_2 implies that $k_{-2} \gg k_3$, which therefore makes $k_4 \approx k_2k_3/k_{-2}$. Thus, eq 10 approximates a preequilibrium step prior to rate-limiting release of H_2 in the second step (eq 11).

With $[DRu_3(CO)_{11}]^-$, the reaction with H_2O under 1 atm of CO liberates HD as the principal dihydrogen product (98%).[3b] The rate of HD evolution from this reaction is very much slower than the reaction of $[HRu_3(CO)_{11}]^-$ (eq 12). It is too slow to be conveniently determined at 25 °C. However, these reactions can be compared at 55 °C: $k_4(H)/k_4(D) \simeq 5$ ($k_4 \simeq 1 \times 10^{-2}$ M^{-1} s^{-1} for $K[HRu_3(CO)_{11}]$ and $k_4 \simeq 2 \times 10^{-3}$ M^{-1} s^{-1} for $K[DRu_3(CO)_{11}]$). The isotope effect ($k_4(H)/k_4(D)$) at 25 °C is expected[53] to be larger than at 55 °C; it is certainly larger than $k_2(H)/k_2(D)$ for eq 10

(45) B_2H_6 reacts with THF to form $THF{\cdot}BH_3$.

(46) (a) Shapley, J. R.; Keister, J. B.; Churchill, M. R.; DeBoer, B. G. *J. Am. Chem. Soc.* **1975**, *97*, 4145. (b) Keister, J. B.; Shapley, J. R. *Inorg. Chem.* **1982**, *21*, 3304.
(47) Partin, J. A.; Richmond, M. G. *J. Organomet. Chem.* **1988**, *353*, C13.
(48) (a) Gladysz, J. A.; Williams, G. M.; Tam, W.; Johnson, D. L. *J. Organomet. Chem.* **1977**, *140*, C1. (b) Casey, C. P.; Neuman, S. M. *J. Am. Chem. Soc.* **1978**, *100*, 2544. (c) Gladysz, J. A.; Tam, W. *Ibid.* **1978**, *100*, 2545. (d) Seinmetz, C. R.; Geoffroy, G. L. *Ibid.* **1981**, *103*, 1278.
(49) Bell, R. P. *The Proton in Chemistry*; Cornell University Press: Ithaca, NY, 1973; pp 258–296.
(50) (a) Rosenberg, E.; Amslyn, E. V.; Barner-Thorsen, C.; Aime, S.; Osella, D.; Gobetto, R.; Milone, L. *Organometallics* **1984**, *3*, 1790. (b) Rosenberg, E. *Polyhedron* **1989**, *8*, 383.
(51) Katakis, D.; Gordon, G. *Mechanisms of Inorganic Reactions*; Wiley-Interscience: New York, 1987; pp 11–14.
(52) Winkler, L. W. *Ber. Dtsch. Chem. Ges.* **1901**, *34*, 1409.
(53) Wiberg, K. B. *Chem. Rev.* **1955**, *55*, 713.
(54) McCarthy, D. A.; Krause, J. A.; Shore, S. G. *J. Am. Chem. Soc.* **1990**, *112*, 8587.
(55) Moore, J. W.; Pearson, R. W. *Kinetics and Mechanism*; Wiley: New York, 1981; p 312, eq 8.95.

at 25 °C (1.4–1.7, Table I). Since the kinetic isotope effect on the overall reaction (eq 12) is larger than the kinetic isotope effect found for eq 10, an additional contribution from k_3 is thereby implied, as expected for the making of an H–H (H–D) bond accompanied by the breaking of an Ru–H (Ru–D) bond.

Acknowledgment. This work was supported by grants from the National Science Foundation (CHE 88-00515 and CHE 84-11630).

Synthesis, Structure, and Reactivity of Cluster Complexes Containing the $Pt_3(\mu_3\text{-Sn})$ Unit and a Possible Relationship to Heterogeneous Platinum–Tin Catalysts

Michael C. Jennings, Guy Schoettel, Sujit Roy, and Richard J. Puddephatt*

Department of Chemistry, University of Western Ontario, London, Ontario, Canada N6A 5B7

Graeme Douglas, Ljubica Manojlović-Muir,* and Kenneth W. Muir

Department of Chemistry, University of Glasgow, Glasgow G12 8QQ, Scotland

Received May 7, 1990

The reaction of $[Pt_3(\mu_3\text{-CO})(\mu\text{-dppm})_3]^{2+}$ (**1**), as the PF_6^- salt, with Me_2SnH_2 gave first $[Pt_3(\mu_3\text{-H})(\mu_3\text{-SnMe}_2H)(\mu\text{-dppm})_3]^{2+}$ (**2**) and then $[Pt_3\{\mu_3\text{-SnMe}_2(O_2PF_2)\}(\mu\text{-dppm})_3]^+$ (**3**) while the reaction of **1** with Ph_3SnH gave $[Pt(\mu_3\text{-CO})(\mu_3\text{-SnF}_3)(\mu\text{-dppm})_3]^+$ (**4a**) and $[Pt_3(\mu_3\text{-Cl})(\mu_3\text{-SnF}_3)(\mu\text{-dppm})_3]$ (**5**). Complexes **4a** and $[Pt_3(\mu_3\text{-CO})(\mu_3\text{-SnCl}_3)(\mu_3\text{-dppm})_3]^+$ (**4b**) could also be prepared by reaction of **1** with SnF_3^- and $SnCl_3^-$, respectively. Reaction of **1** with excess SnF_3^- or $SnCl_3^-$ gave $[Pt_3(\mu_3\text{-SnF}_3)_2(\mu\text{-dppm})_3]$ (**6a**) or $[Pt_3(\mu_3\text{-SnCl}_3)_2(\mu\text{-dppm})_3]$ (**6b**), respectively. The structure of **6a** has been determined by X-ray crystallography. Reaction of **4a** with acetylene in CH_2Cl_2 gave an equimolar mixture of $[Pt_3Cl(\mu_3\text{-HCCH})(\mu\text{-dppm})_3]^+$ (**8**) and **6a**, reaction with H_2S gave $[Pt_3H(\mu_3\text{-S})(\mu\text{-dppm})_3]^+$ (**9**) and SnS, and reaction with XyNC (Xy = 2,6-$Me_2C_6H_3$) gave $[Pt_3(\mu_3\text{-SnF}_3)(\text{XyNC})(\mu\text{-dppm})_3]^+$ (**7**), which contains a terminal XyNC ligand. The stability of the $Pt_3(\mu_3\text{-SnX}_3)$ unit, together with the ability of the coordinatively unsaturated Pt_3 clusters to mimic properties of a Pt surface, suggests that heterogeneous Pt–Sn–Al_2O_3 catalysts may contain platinum–tin alloy anchored to the tin(II)–alumina support by similar $Pt_3(\mu_3\text{-Sn})$ linkages. An ESCA study of the complexes suggests that SnF_3^- is a stronger σ-donor than CO but also competes with CO as a π-acceptor ligand.

Introduction

Bimetallic Pt–Sn systems are involved in both homogeneous and heterogeneous catalysis.[1-6] Molecular Pt(II)–Sn(II) complexes take part in homogeneous catalytic hydrogenation, hydroformylation, and isomerization of alkenes.[2-6] Most of these compounds contain the $SnCl_3^-$ ligand.[1-9] Heterogeneous Pt–Sn–Al_2O_3 catalysts are used in re-forming of petroleum since they give higher selectivity for isomerization and aromatization than Pt–alumina catalysts alone. They appear to contain both Sn(0) and Sn(II) species, but the origin of the tin effect is not clearly established.[10-19]

Scheme I

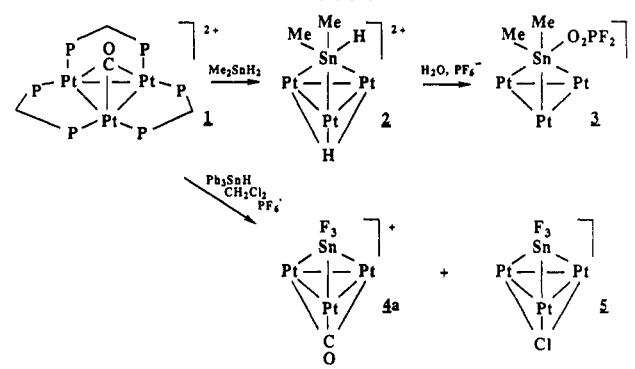

(1) Holt, M. S.; Wilson, W. L.; Nelson, J. H. *Chem. Rev.* **1989**, *89*, 11.
(2) Cramer, R. D.; Jenner, E. L.; Lindsey, R. V., Jr.; Stolberg, U. G. *J. Am. Chem. Soc.* **1963**, *85*, 1691.
(3) Anderson, G. K.; Clark, H. C.; Davies, J. A. *Inorg. Chem.* **1983**, *22*, 427, 434, 439.
(4) Anderson, G. K.; Clark, H. C.; Davies, J. A. *Organometallics* **1982**, *1*, 64.
(5) Hsu, C.; Orchin, M. *J. Am. Chem. Soc.* **1975**, *97*, 3553.
(6) Kawabata, Y.; Hayashi, T.; Ogata, I. *J. Chem. Soc., Chem. Commun.* **1979**, 462.
(7) Herbert, I. R.; Pregosin, P. S.; Ruegger, H. *Inorg. Chim. Acta* **1986**, *112*, 29. Arz, C.; Herbert, I. R.; Pregosin, P. S. *J. Organomet. Chem.* **1986**, *308*, 373.
(8) Albinati, A.; Moriyama, H.; Ruegger, H.; Pregosin, P. S.; Togni, A. *Inorg. Chem.* **1985**, *24*, 4430. Reugger, H.; Pregosin, P. S. *Inorg. Chem.* **1987**, *26*, 2912.
(9) Grossel, M. C.; Moulding, R. P.; Seddon, K. R. *Inorg. Chim. Acta* **1982**, *64*, L275.
(10) Adkins, S. R.; Davis, B. H. *J. Catal.* **1984**, *89*, 371.
(11) Davis, B. H. *J. Catal.* **1976**, *42*, 376; **1977**, *46*, 348.
(12) Burch, R.; Garla, L. C. *J. Catal.* **1981**, *71*, 360.
(13) Davis, B. H.; Westfall, G. A.; Watkins, J.; Pezzarite, J., Jr. *J. Catal.* **1976**, *42*, 247.

0276-7333/91/2310-0580$02.50/0